



Geochronological Evidence of Pan-African Eclogites from the Central Menderes Massif, Turkey

ROLAND OBERHÄNSLI¹, OSMAN CANDAN² & FRANZISKA WILKE¹

¹Institut für Erd- und Umweltwissenschaften, Universität Potsdam, Karl-Liebknecht Strasse 24,
Potsdam 14476, Germany (E-mail: roob@geo.uni-potsdam.de)

²Dokuz Eylül University, Engineering Faculty, Department of Geological Engineering, Buca, TR–35100 İzmir, Turkey

Received 20 January 2010; revised typescript receipt 03 February 2010; accepted 08 February 2010

Abstract: The Menderes Massif in western Anatolia documents a complex geodynamic history from Precambrian to recent. Eclogitic relics found in metagabbros in the Precambrian basement were dated by the U/Pb method. The zircon age data from granulitic (coronitic) and eclogitic metagabbros is consistent with geological constraints as well as relative and radiometric ages of the host granulitic gneisses and augen gneisses. A Pan-African intrusion age (540 Ma) of the metagabbros and a shortly later eclogite facies event (530 Ma) are inferred. This scenario fits with the geodynamic evolution deduced from the acidic country rocks of the eclogitic metagabbros. Direct links between the Menderes Massif and Mozambique belt are obliterated by Alpine deformation. Nevertheless, the tectonic setting and age of the Menderes eclogites support a terminal collision of East and West Gondwana and the final suturing of the Mozambique Ocean during the Early Cambrian.

Key Words: Menderes Massif, eclogites, Pan-African metamorphism, zircon U/Pb ages, Mozambique belt

Menderes Masifi'nin Orta Kesimindeki Pan-Afrikan Eklojitlerine Ait Jeokronolojik Veriler

Özet: Batı Anadolu'da yer alan Menderes Masifi Prekambriyen'den günümüze uzanan karmaşık bir jeodinamik geçmişe ait veriler içerir. Prekambriyen temelinde bulunan, metagabrolarla ilişkili eklojitik kalıntılar U/Pb yöntemiyle yaşlandırılmıştır. Granulitik (koronitik) ve eklojitik metagabrolardan elde edilen yaşlar, genel jeolojik verilerin yanı sıra çevre kayayı oluşturan granulitik gnays ve gözlü gnaysların göreceli ve radyometrik yaşları ile de uyum sunmaktadır. Veriler, gabro sokulumlarının Pan-Afrikan (540 My) yaşlı olduğunu ve izleyen evrede (535 My) eklojit fasiyesi koşullarında başkalaşıma uğradıklarını göstermektedir. Bu senaryo, eklojitik metagabroların çevre kayalarını oluşturan asidik magmatiklerin jeodinamik evrimleri ile uyum göstermektedir. Menderes Masifi ile Mozambik kuşağı arasındaki doğrudan ilişkinin Alpin deformasyonu ile büyük oranda silinmiş olmasına karşın söz konusu eklojitlerinin yaş ve tektonik ortamının Erken Kambriyen'de Doğu ve Batı Gondwana'nın çarpışması ve Mozambik Okyanusu'nun kenetlenmesi evresini tanımladığı düşünülmektedir.

Anahtar Sözcükler: Menderes Masifi, eklojit, Pan-Afrikan metamorfizması, zircon U/Pb yaşları, Mozambik kuşağı

Geologic Frame of the Menderes Massif

The region of Western Turkey underwent complex Pan-African, Variscan and Alpine orogenic processes involving accretion of various terranes and microcontinents. Associated with these processes, continental and oceanic crusts were subducted and exhumed. Age determinations of discrete

petrological assemblages that can be tied to specific geodynamic processes are therefore crucial for a better understanding of the geological evolution of the region.

The evolution of the Menderes Massif comprises at least six prograde as well as retrograde metamorphic phases and four magmatic cycles

(Dürr 1975; Satir & Friedrichsen 1986; Candan *et al.* 1994, 2001; Candan 1996a, b; Bozkurt & Oberhänsli 2001). The simple core-cover interpretation for the Menderes Massif has been discarded and a complex nappe structure proposed (Figure 1; Partzsch *et al.* 1998; Ring *et al.* 1999a, b; Gessner *et al.* 2002). Further investigation showed that the Menderes core (crystalline basement) consists of separate Pan-African and Palaeozoic units (Candan *et al.* 2001; Dora *et al.* 1995). The Pan-African rocks of the central complex of the Menderes Massif show a poly-metamorphic evolution (Candan *et al.* 2001) and contain eclogitic metagabbros and eclogites (Oberhänsli *et al.* 1997; Candan *et al.* 2001; Warkus 2001). The high-pressure rocks are restricted to the strongly metamorphosed Precambrian basement of the Massif.

Contacts of some metagabbros show they intruded the enclosing country rocks (Oberhänsli *et al.* 1997). The metagabbros occur as lenses parallel to the main foliation of the encasing gneisses and are commonly zoned.

Near Birgi (Figure 1), the cores of such lenses exhibit magmatic granoblastic textures. Generally they show coronitic textures typical of an early prograde amphibolite to granulite facies metamorphism (Candan *et al.* 2001). Along shear bands, however, these earlier high temperature parageneses were replaced by eclogite facies parageneses (Figure 2). The enclosing paragneisses, orthogneisses and migmatites yield Pan-African ages (Table 1) (e.g., Hetzel *et al.* 1995; Hetzel & Reischmann 1996; Loos & Reischmann 1999; Warkus 2001). Similar ages (540 to 580 Ma) have been reported from the northern and southern complexes of the Menderes Massif (e.g., Dannat 1997; Gessner *et al.* 2004; Catlos & Çemen 2005). In this paper we present new geochronological data from the eclogites of the Menderes Massif. Moreover, based on the observed ages we discuss the geodynamic link between the Menderes Massif and the Mozambique belt.

Geology and Petrology of Eclogite Locations

In the Ödemiş-Kiraz and Aydın mountains of the central Menderes Massif, metagabbros with high-

pressure relics occur within the basement consisting of orthogneisses and high-grade schists / paragneisses (Figure 1). Eclogitic relics have been observed at Salihli, Alaşehir, Birgi, Kiraz and Tire (Oberhänsli *et al.* 1997; Candan *et al.* 2001). Yet, from the northern part of the Menderes Massif (Simav complex) eclogites were reported from only a few localities (Candan *et al.* 2001), while in the southern Menderes Massif (Çine complex) eclogitic relics have not been observed, though metagabbros are widespread. In the central Menderes Massif (Salihli, Alaşehir, Birgi, Kiraz, Tire) eclogitic metagabbros are more abundant. Well-preserved eclogites recrystallized from a basaltic protolith were recognized near Kiraz.

Field observation in the Pan-African basement of the Menderes Massif and thin section studies show a complex polyphase metamorphic history. There is evidence that the eclogite stage overprints a coronitic upper amphibolite to granulite stage and both the coronitic and eclogitic stages were overprinted by a later amphibolite-facies event (Candan *et al.* 2001). Granulite facies relics such as orthopyroxene and sillimanite occur in the surrounding orthogneisses (Dora *et al.* 1995; Candan *et al.* 2001). Based on these observations several P-T paths have been shown (Figure 3), proposing an evolution from granulite facies to eclogite facies followed by almost isothermal decompression producing an amphibolite facies overprint (Oberhänsli *et al.* 1997; Partzsch *et al.* 1998; Candan *et al.* 2001). Evidence for an eclogitisation after the granulite stage includes textural evidence such as a coronitic gabbro with an eclogitic vein (Figure 2) that indicates that recrystallisation took place along with fluid circulation.

Warkus (2001) made the first attempts to date zircons from the eclogitic metagabbro of Alaşehir using the Pb-Pb evaporation method. 10 zircons were analysed. Two single zircon analyses and a bulk of 8 grains show ages ranging between 507 ± 4 Ma, 497 ± 6.2 Ma and 521 ± 1.9 Ma. In this study we used zircons from eclogitic samples from Birgi, Kiraz, and Tire for dating. The Salihli samples could not be dated due to inadequate zircon content.

The *Birgi region* (Figure 4) is characterised by a widespread occurrence of small and large gabbroic to

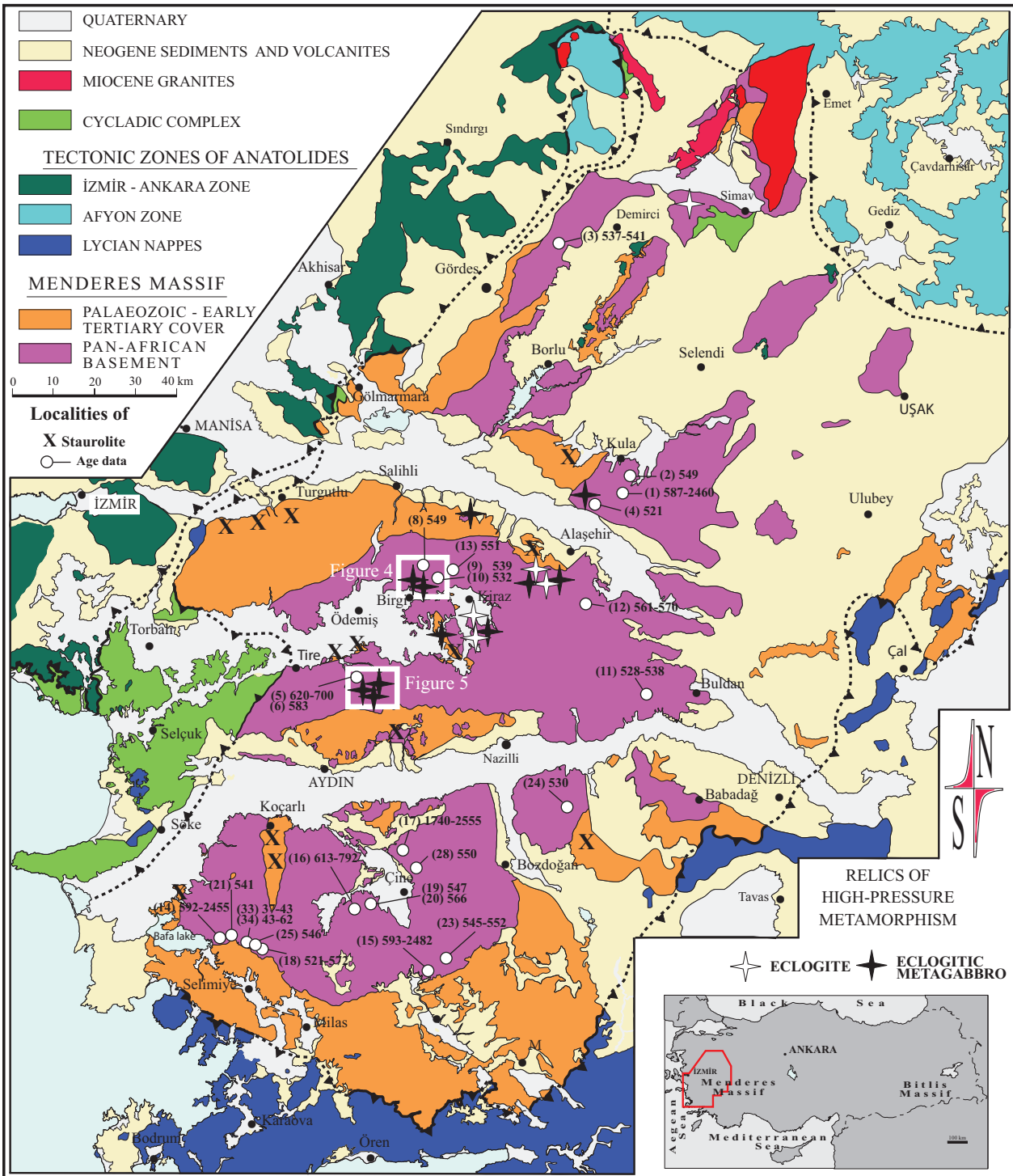


Figure 1. Generalised geologic map of the Menderes Massif and the main localities of the Pan-African high-pressure relics (modified after Candan et al., 2001). The Massif can be divided into three major submassifs, the Simav-Gördes complex to the North, the Ödemiş-Kiraz complex in the Centre and Çine complex to the south. White points with numbers in parenthesis indicate locations for ages given in Table 1. Due to imprecise location 9 references are not plotted.

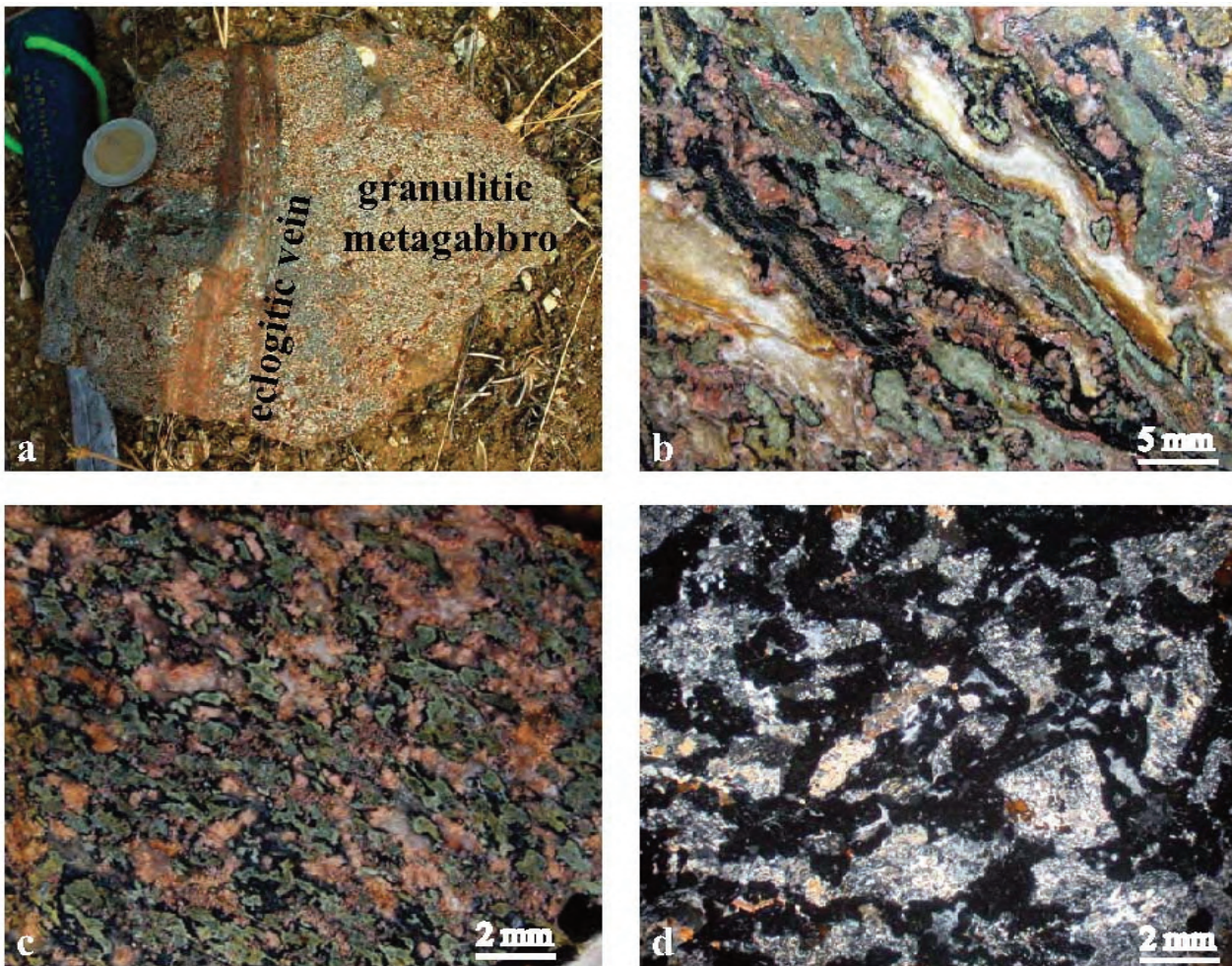


Figure 2. (a) Photograph showing the effect of fluid infiltration and deformation resulting in eclogitization of the coronitic metagabbro in the Birgi locality; (b) hand specimen view of a coronitic metagabbro; (c) hand specimen view of eclogitic metagabbro showing relic plagioclase and the omphacite (light green) + garnet association; (d) microphotograph of eclogitic metagabbro showing ghost textures of relict magmatic plagioclase.

amphibolitic stocks and lenses within augen- and para-gneisses. The largest bodies consist of gabbroic protoliths with relict magmatic granoblastic textures (Oberhänsli *et al.* 1997; Candan *et al.* 2001; Warkus 2001) that are superimposed by coronitic textures, indicating a high temperature metamorphic event. Along their strongly deformed marginal zones, the coronitic metagabbros have been transformed to eclogite and finally to amphibolites. In the undeformed cores of metagabbroic lenses the relict igneous mineral assemblage consists of plagioclase, hornblende, orthopyroxene, clinopyroxene and

rarely olivine. Accessory secondary minerals are titanite, biotite and white mica. Very fine-grained coronitic textures with amphibole, biotite, garnet and clinozoisite demonstrate a first HT metamorphic overprint of these rocks. Along crosscutting shear bands symplectitic textures (omphacite, plagioclase, quartz) dominate. Larger veins contain eclogitic assemblages with garnet, omphacite and quartz. Plagioclase remains as a relict phase enclosed by garnet (Figure 2). For dating we separated zircons from eclogitic veins and eclogitic metagabbros.

Table 1. Compilation of age data available from the Menderes Massif basement rocks. Numbers for identification are used on Figure 1.

	Lithology / Locality	Method	Age (Ma)	Authors
Demirci-Gördes (northern) Submassif				
1	paragneiss, Kula	Pb/Pb single-zircon evaporation	2460–587	Dora <i>et al.</i> 2002
2	orthogneiss, Kula	Pb/Pb single-zircon evaporation	549.7±7.6	Dora <i>et al.</i> 2002
3	orthogneiss, Simav orthogneiss, Demirci	Pb/Pb single-zircon evaporation	541.4±2.5 537.2±2.4	Dannat 1997
4	metagabbro, Alaşehir	Pb/Pb single zircon evaporation	521±1.9	Warkus 2001
Ödemiş-Kiraz (central) Submassif				
5	granulite, Tire	monazite U/Th/ Pb microprobe	620–700	Warkus 2001
6	granulite, Tire	U/Pb SHRIMP	583.0±5.7	Koralay <i>et al.</i> 2006
7	garnet schist, Alaşehir	monazite, U/Th/ Pb microprobe	512–483	Catlos & Çemen 2005
8	paragneiss, Birgi	Pb/Pb single-zircon evaporation	622–2558	Dora <i>et al.</i> 2002
9	orthogneiss, Birgi	zircon	539±9	Warkus 2001
10	orthogneiss, Birgi	monazite	532±19	Warkus 2001
11	orthogneiss, Kuyucak orthogneiss, Buldan orthogneiss, Kiraz	Pb/Pb single-zircon evaporation	528.0±4.3 528.1±1.6 538.1±2.6	Dannat 1997
12	orthogneiss, Alaşehir	Pb/Pb single-zircon evaporation	561.5±0.8 570.5±2.2	Koralay <i>et al.</i> 2004
13	migmatite-metagranite, Birgi	U/Pb	551±1.4	Hetzel <i>et al.</i> 1998
Çine (southern) Submassif				
14	mica schist, Bafa	Pb/Pb single-zircon evaporation	592–2455	Dora <i>et al.</i> 2005
15	mica schist, Yatağan	Pb/Pb single-zircon evaporation	593–2482	Dora <i>et al.</i> 2005
16	paragneiss, Çine	Pb/Pb single-zircon evaporation	792–613	Dora <i>et al.</i> 2002
17	paragneiss, Çine	Pb/Pb single-zircon evaporation	2555–1740	Reischmann <i>et al.</i> 1991
18	orthogneiss, Selimiye	Pb/Pb single-zircon evaporation	563±3, 536±9 572±7, 521±8 556±4, 546±5 551±5	Loos & Reischmann 1999
19	orthogneiss, Çine	Pb/Pb single-zircon evaporation	547.2±1.0	Gessner <i>et al.</i> 2001
20	orthogneiss, Çine	U/Pb SHRIMP	566±9	Gessner <i>et al.</i> 2004
21	orthogneiss, Bafa	U/Pb SHRIMP	541±14	Gessner <i>et al.</i> 2004
22	orthogneiss, Çine	Rb/Sr whole rock	490±90	Dora (1975, 1976)
23	orthogneiss, Yatağan	Pb/Pb single-zircon evaporation	552.1±2.4 551.5±2.9 545.6±2.7	Dora <i>et al.</i> 2005
24	orthogneiss, Karacasu	Pb/Pb single-zircon evaporation	530.9±5.3	Koralay <i>et al.</i> 2007
25	orthogneiss, Selimiye	Pb/Pb single-zircon evaporation	546.0±1.6 546.4±0.8	Hetzel & Reischmann 1996
26	orthogneiss, Çine	Rb/Sr whole rock	471±9	Satir & Friedrichsen 1986
27	garnet gneiss, Çine	monazite, U/Th/ Pb microprobe	571, 488, 437	Catlos & Çemen 2005
28	migmatite, Çine	Pb/Pb single-zircon evaporation	~540	Dannat 1997
29	migmatite, Çine	Rb/Sr whole rock	~529	Schuiling 1973
30	migmatite, Çine	Rb/Sr whole rock	502±10	Satir & Friedrichsen 1986
31	orthogneiss, Çine	Rb/Sr biotite Rb/Sr white mica	37±1 56±1	Satir & Friedrichsen 1986
32	orthogneiss, Aydın	Ar/Ar white mica	36±2	Lips <i>et al.</i> 2001
33	orthogneiss, Selimiye	Ar/Ar white mica	43–37	Hetzel & Reischmann 1996
34	quartz vein, Selimiye	Rb/Sr white mica	62–43	Bozkurt & Satir 2000

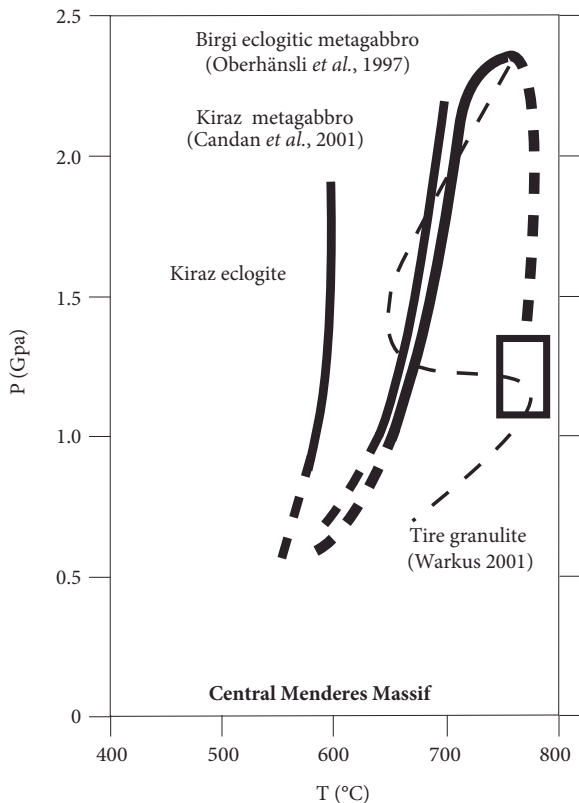


Figure 3. Compilation of published P-T evolutions for the eclogitic rocks of the Central Menderes Massif. The problem of a pre- versus post-eclogitic granulite stage is discussed in the text. A pre-eclogite granulite stage is supported by textural arguments (see text and Figure 2a).

Kiraz is the only locality with both eclogitic metagabbros and eclogites with basaltic precursors. Both eclogitic rock types are in contact with augen gneisses and mica schists. The basaltic eclogites are fresh and show synmetamorphic folding, whereas the eclogitic metagabbros are strongly altered. Eclogites are composed of garnet, omphacite and rutile. Plagioclase occurs as a relict phase and amphibole as a post HP mineral. Additionally ilmenite, zoisite and quartz occur.

In the *Tire Klippe* (Figure 5), eclogitic metagabbros are associated with granulites and migmatites (Oberhänsli *et al.* 1997). Typical primary lithologies of the metabasic igneous rocks are olivine gabbros, noritic gabbros and norites. As in the Birgi region, igneous precursors with subophitic to holocrystalline texture are well preserved in the cores

of the bodies. Eclogitic metagabbros are better preserved than in the Birgi region. They are composed of garnet, rutile, omphacite, quartz and amphibole, and contain accessory epidote, biotite, chlorite and zircon. Zircon occurs preferentially as inclusions in quartz.

Material and Methods

Material

10 eclogite samples were selected for zircon U/Pb analyses. Five samples, one eclogitic metagabbro (361), one coronitic gabbro (362) and three eclogites with basaltic protolith (363, 364, 365) are from the Birgi-Kiraz area. One sample of eclogitic metagabbro was taken from the Tire Klippe (370). The Kiraz samples had to be rejected since no zircon could be separated from samples 363 and 364, and sample 365 contained <1% zircon. The two Birgi samples (361, 362) contained enough zircon for age determination.

Sample Preparation

Samples were crushed and sieved and heavy minerals separated on a water table. Magnetic minerals were separated with a FRANZ magnetic separator with currents of 0.6, 0.9 at an inclination of 10° and 1.2 A at 5°. Diamagnetic minerals were sampled at the last step, then bromoform [CHBr₃] and diiodinemethane [CH₂I₂] were used as heavy liquids. The concentrates were checked for zircon, rutile, titanite and apatite under immersion liquids.

Zircon was hand-picked and analysed with a scanning electron microscope (JEOL 840, Centraurus-BSE/CL, OXFORD INCA EDX; University Münster) and by cathodoluminescence (CL, CL8200mk4; University Potsdam).

TIMS Isotope Analyses

The chemical treatment for isotope analyses is based on the method of Krogh (1973). For cleaning, hand-picked zircons were placed in 3ml Savillex[®]-Teflon crucibles. 1ml 6N HCl and 2 drops of HNO₃ were added. The crucibles were left overnight on a 90 °C hot plate and then the contents washed 4 times with distilled water. For digestion, 50 mg of the ²⁰⁵Pb-²³⁵U

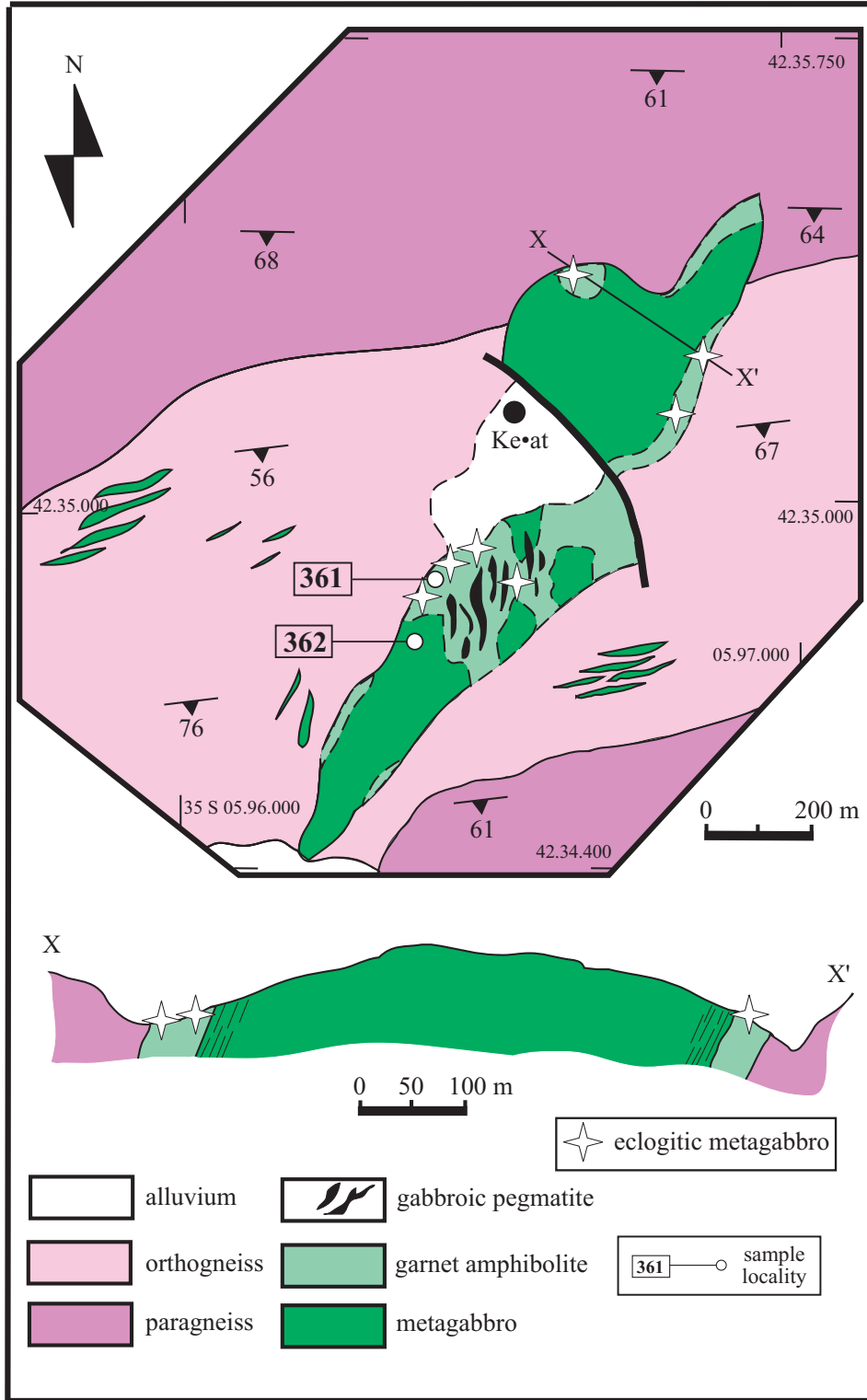


Figure 4. Geological sketch map and cross section of the Birgi area showing amphibolitic and metagabbroic lenses within the augen gneisses of the Panafrican basement (modified after Candan 1996a). For regional location see Figure 1.

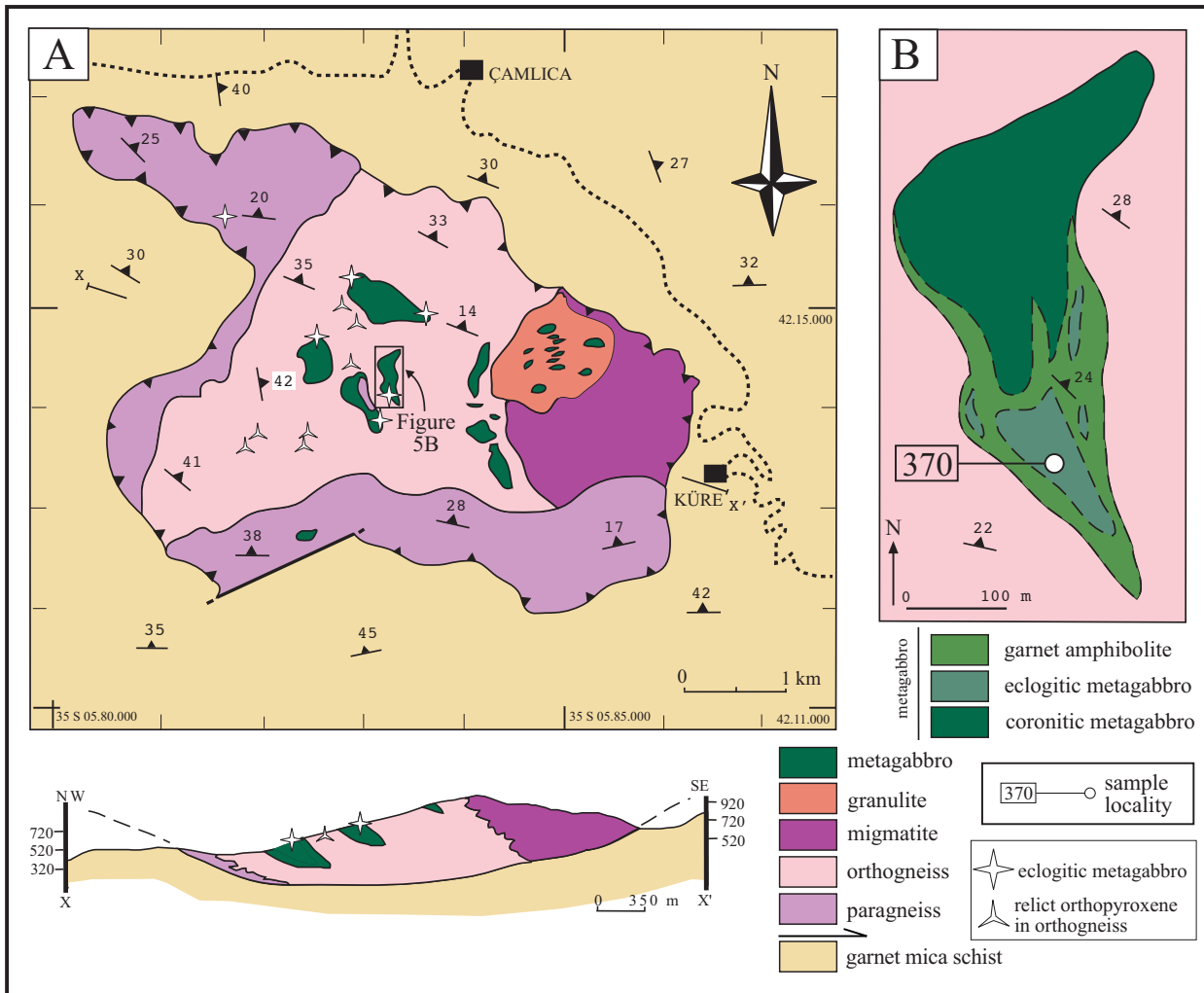


Figure 5. Geological sketch maps and cross-section of the Tire klippe and the eclogitic metagabbro occurrence (modified after Çetinkaplan 1995). For regional location see Figure 1.

spike were added together with 1 ml 24N HF and 3 drops concentrated HNO_3 . Distilled water was added so as not to cover the bottom of the crucibles completely. The Savillex[®]-Teflon beakers were placed in Parr[®]-bombs and left for 5 days at 200 °C. After optical control the samples had to be treated in the same way for another 10 days. A second set of the same samples needed 3 weeks for digestion. The samples were then condensed at 80–90 °C and taken up with ca. 0.5 ml 3N HCl. For the separation of U and Pb, resin filled (Bio-Rad AG 1x 8, 100–200 mesh) Teflon columns with a volume of ca. 200 μl were used. They were cleaned with 1 reservoir volume

(RV) distilled water, and 1 RV 6N HCl and finally equilibrated with 0.75 RV 3N HCl. The columns were loaded with the samples and washed twice with 0.75 RV 3N HCl. After extraction of the 3N HCl, Pb and U were eluted with 0.75 RV 6N HCl and 0.75 RV H_2O respectively. The elutes were taken up in HNO_3 conc. and 1 drop of H_3PO_4 and completely dried on a 90 °C hot plate. H_3PO_4 marks the sample since it does not evaporate.

The samples were then transferred to Refilaments following the method of Cameron *et al.* (1969). To determine the external reproducibility of the isotope

ratios standard NBS 982 with a concentration of 30 ppm was used for Pb and standard U-500 with a concentration of 250 ppm for U. To enhance measurements 1 μ l H_3PO_4 was added to both standards. U was measured as double oxide $^{267}UO_2^{2+}/^{270}UO_2^{2+}$.

Isotope ratios were measured with a VG Sector 54 Multicollector Thermion-mass spectrometer (TIMS) at the Central Laboratory for Geochronology, University of Münster.

Samples were measured with Faraday collectors, except for sample 370 which was analysed with an ion detector (Daly). Measurements of standards started every experiment. Decay constants after Jaffey *et al.* (1971) were used as suggested by Steiger & Jäger (1977). For data processing we used Pb-DAT 1.24 (Ludwig 1980) and ISOPLOT.

Cathodoluminescence

The coronitic metagabbros from Birgi contain zircons (362c, d) with unzoned cores and a very thin metamorphic rim (Figure 6a, b). Both samples show only thin bright edges that represent the metamorphic overgrowth, making up approximately 10% of the crystals. Zircons from the eclogitic metagabbros of Birgi and Tire (Figure 6c, d) mostly show dark, mainly unzoned cores. Samples 370f and 361c are overgrown with double rims, reflecting metamorphic episodes. Sample 370f from Tire exhibits sector zoning around a homogeneous core that we assign to a first metamorphic event (M1). The Birgi sample (361c) has cracked cores and a continuous zoned growth pattern assigned also to M1. The second metamorphic event (M2) produced small bright rims. All rims are prismatic and thus must be interpreted to have grown at least under upper amphibolite facies conditions (Vavra *et al.* 1999). Despite the variability shown, we did not abrade zircons due to their small size and their complex growth pattern.

TIMS Analyses

From the *Birgi coronitic metagabbro* we picked 25 to 30 crystals of homogeneous yellowish to clear zircon, 150 μ m in diameter, for two measurements. Sample

362 gives a concordant age of 540.4 ± 3.5 Ma (Figure 5a). The $^{206}Pb/^{238}U$, $^{207}Pb/^{235}U$, and $^{207}Pb/^{206}Pb$ ages are 540 ± 4 Ma, 541 ± 3 Ma and 543 ± 8 Ma, respectively (Table 2).

From the *Birgi eclogitic metagabbro* we prepared a first batch (361a) consisting of 25 yellowish clear idiomorphic zircons (100 μ m) and a second batch (361b) with 100 smaller but optically identical zircons. Both samples revealed concordant ages of 529.9 ± 22 Ma (Table 2; Figure 5b) but the $^{206}Pb/^{204}Pb$ ratio of sample b indicates less inherited Pb. A small correction (Stacey & Kramers 1975) thus put sample 361b on the Concordia as well. We assume a small but significant effect of the inherited cores. The cathodoluminescence study infers a small loss of Pb due to metamorphism or hydrothermal leaching. The low Pb content of our samples and hence the large effect of estimated inherited Pb (Stacey & Kramers 1975) hampers our analyses. Since feldspar is missing in the high pressure paragenesis of these samples, the method to determine common Pb analytically on feldspar (e.g., Möller *et al.* 2000) could not be applied.

From the *Tire eclogitic metagabbro* we analysed 75 colourless to yellowish idiomorphic to rounded zircons (350 μ m; sample 370b). ^{204}Pb values were close to instrumental detection limits and the sample is not considered in the discussion. The data of 25 grains from sample 370a are discordant. The samples contain a high amount of inherited Pb as can be seen from the $^{206}Pb/^{204}Pb$ ratio (Table 2, Figure 5c). Besides estimating inherited Pb (Stacey & Kramers 1975), an additional correction is needed. Influence from the inherited core and/or Pb loss cannot be excluded. Extremely long digestion times in HF and the colours in CL images point to U-poor zircons similar to sample 370b. Zircons (370a) are not metamict and therefore Pb loss should not be an important factor. Based on inherited Pb and inherited cores we interpret a $^{206}Pb/^{238}U$ age of 531 ± 9 Ma as a minimum age for this sample.

Consequences for the Metamorphic Evolution

We will summarise below geological, petrological and geochronological evidence for the Pan-African and Alpine orogenic events that have influenced the

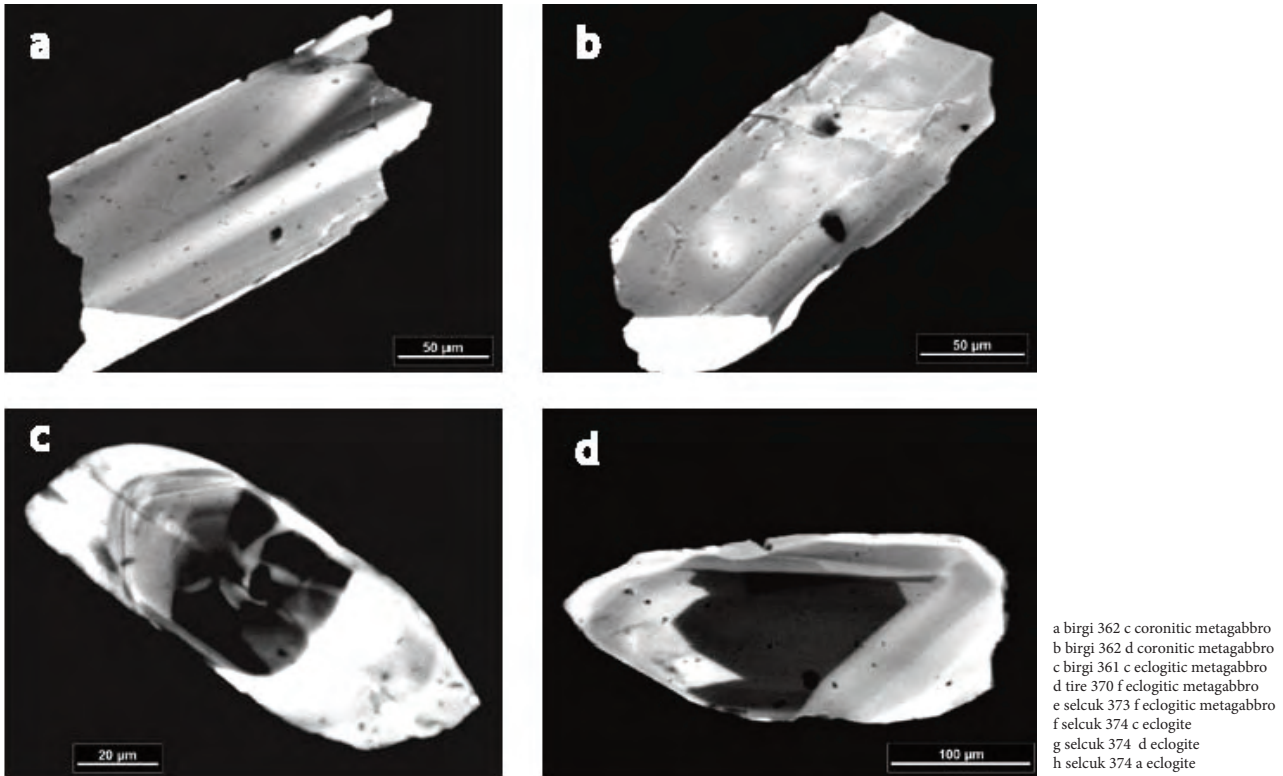


Figure 6. CL images of Birgi and Tire metagabbros: (a, b) Birgi coronitic metagabbro (samples 362c, d): broken zircons crystals with poly-faceted core surrounded by fine sector zoned light rims; (c) Birgi eclogitic metagabbro (sample 361 c): long prismatic zircon with resorbed core surrounded by a light rim with sector zoning; (d) Tire eclogitic metagabbro (sample 370 f): broken prismatic core surrounded by a rim with lamellar sector zoning. The rim shows chemical resorption features.

investigated zircons. We will discuss the new ages with respect to the zoning pattern of the zircons, since bulk analyses of zoned crystals produce mixing ages. Zonation pattern and habits determine the extent of mixing of ages. Finally we will compare radiometric data from surrounding gneisses and migmatites with zircon ages from the eclogitic rocks.

Effects of Pan-African and Alpine Orogenesis

The Pan-African basement is unconformably overlain by a Palaeozoic series of metamorphic rocks containing chloritoid, garnet and staurolite, indicating that both Precambrian basement and its sedimentary cover series underwent post Pan-African upper greenschist to lower amphibolite facies metamorphism. $^{40}\text{Ar}/^{39}\text{Ar}$ mica ages from the whole Menderes Massif, including crystalline basement and metasedimentary cover, show

identical Alpine ages, indicating that the entire Menderes Massif was heated above the blocking temperatures of mica during the Eocene. This means also that the basement must have been heated above the closure temperature of white mica (500 ± 50 °C Rb-Sr; 350 ± 50 °C K-Ar, Ar/Ar). All these facts point to elevated temperatures during the Alpine orogeny. Furthermore, migmatites and related granites are common in the Menderes Massif. With the exception of the Demirci area at the northern limit of the Simav-Gördes complex (Oligocene–Early Miocene migmatites; Bozkurt pers. comm.), migmatites are restricted to the Pan-African basement. This observation is consistent with geochronological data from acidic rocks (Gessner *et al.* 2004; Koralay *et al.* 2006). SHRIMP U/Pb analyses from the outermost rims of zircons from metagranites of the Çine region (Gessner *et al.* 2004) have not yielded young (Alpine) ages. This suggests that zircons from the Pan-African basement in the Ödemiş-Kiraz and Çine complexes

Table 2. U/Pb isotope data from zircons of eclogitic and coronitic metagabbros of the Birgi and Tire region.

sample	rocktype	common Pb ²⁺ [ppm]	ratios						ages [Ma]			discordance ³ [%]				
			²⁰⁶ Pb/ ²⁰⁴ Pb	²⁰⁷ Pb/ ²⁰⁶ Pb	err	²⁰⁷ Pb/ ²³⁵ U	err	²⁰⁶ Pb/ ²³⁸ U	err	age	err		age	err		
Birgi																
362a	coronitic metagabbro	20	1345	0.05836	0.00021	0.70278	0.00562	0.08734	0.00061	540	4	541	3	543	8	(-0.65)
362b	coronitic metagabbro	0.0096	114	0.06065	0.00411	0.73104	0.10673	0.08742	0.01128	540	67	557	63	627	147	(-13.82)
361a	metagabbro	23	135	0.05911	0.00250	0.70953	0.05392	0.08706	0.00548	538	33	545	32	571	92	(-5.77)
361b	metagabbro	0.54	600	0.05871	0.00055	0.68603	0.01441	0.08474	0.00153	524	9	530	9	557	21	(-5.77)
Tire																
370a	metagabbro	87	192	0.06229	0.00059	0.73697	0.01473	0.08582	0.00146	531	9	561	8	684	20	-22.39
370b	metagabbro	0.0027	886	0.06013	0.00123	0.60910	0.04873	0.07347	0.00566	457	34	483	31	608	44	-24.88

* corrected for spike, blank, common lead (after Stacy & Kramers 1977) and mass fractionation

° measured ratio

² blank not considered³ gives distance to concordia. discordance = (²⁰⁶Pb/²³⁸U age / (²⁰⁷Pb/²⁰⁶Pb age / 100)) - 100 (Möller *et al.* 2000)**Sample coordinates:**

Birgi eclogitic metagabbro

Birgi coronitic metagabbro

Tire eclogitic metagabbro

35 S 05 96412 / 42.34825

35 S 05 96435 / 42.34740

35 S 05 83112 / 42.13852

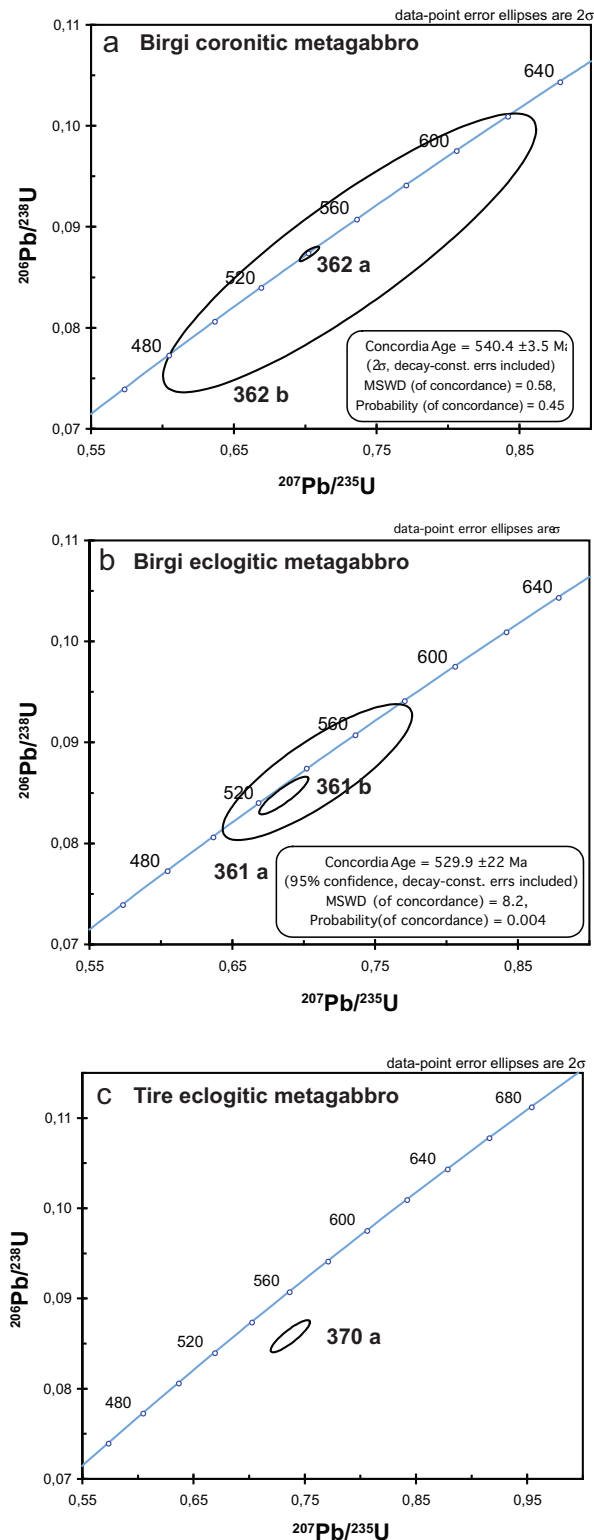


Figure 7. U/Pb concordia diagrams; (a) Birgi coronitic metagabbro; (b) Birgi eclogitic metagabbro; (c) Tire eclogitic metagabbro; for discussion see text.

have not been affected by Alpine high temperature events.

In the central Ödemiş-Kiraz complex, a polyphase Pan-African evolution with granulite, eclogite and amphibolite facies metamorphism is based on petrological (Oberhänsli *et al.* 1997; Candan *et al.* 2001), as well as on geochronological data from the augen gneiss (Warkus 2001; Oberhänsli *et al.* 2002). Eclogitic metagabbros occur only within the Pan-African basement of the Central Menderes Massif. No evidence for an eclogitic metamorphism in the kyanite-staurolite-garnet-bearing Palaeozoic metasediments has been observed.

In the southern Çine complex, metagabbros within the Pan-African basement have experienced neither the eclogite nor the granulite overprint. Most of the Menderes Massif Pan-African basement experienced lower amphibolite facies metamorphism. Migmatites and related granite intrusions only occur within the Pan-African basement. In the Çine-Yatağan area (southern Menderes Massif) the Pan-African basement is unconformably overlain by Palaeozoic metasediments with a basal metaconglomerate. In the Koçarlı and Bozdoğan area these Palaeozoic series contain schists with kyanite, staurolite and garnet representing lower amphibolite facies conditions. Along the southern edge of the Menderes Massif, between Selimiye and Yatağan, the Palaeozoic schists include phyllites with garnet and chloritoid, recording upper greenschist facies conditions. This indicates that during the Alpine event, temperatures never reached upper amphibolite facies conditions in the cover rocks. The Triassic to Palaeocene series along the southern margins of the Menderes Massif records HP/LT metamorphism (Rimmelé *et al.* 2003; Whitney *et al.* 2008) during an Alpine event. To summarise, petrological evidence of the polyphase Pan-African metamorphism and relative age relations suggest a granulite-eclogite-upper amphibolite evolution, whereas the Alpine events indicate a blueschist and upper greenschist facies overprint along the southern border of the Menderes Massif while to the north lower amphibolite conditions are recorded.

Complex Zircon Zoning Pattern

Zircons dated from eclogites show complex zoning textures, representing a complex magmatic and polymetamorphic history. CL images of the Menderes eclogite zircons reveal a polyphase history with a magmatic stage (broken cores) that was followed by a first metamorphic event (M1) that produced major portions of sector zoning. Furthermore, all zircons show small, bright metamorphic rims, which we assign to a second metamorphic event (M2). As shown on the CL images (Figure 4), the major portion of the zircon crystals is made up of sector-zoned parts. Such sector zoning is typical of amphibolite to granulite facies metamorphic conditions (Vavra *et al.* 1999). Therefore we are confident that the ages retrieved from zircons in eclogitic metagabbros represent the timing of the eclogite-upper amphibolite transition, which might have resulted in migmatization and granite generation. This event was brief, as deduced from petrological and geological observations (Oberhänsli *et al.* 1997; Candan *et al.* 2001) and supported by ages (Koralay *et al.* 1998; Hetzel *et al.* 1998). Yet we are aware that both Pan-African and Alpine events could have produced these complex zircon patterns, since both orogenic events led to amphibolite facies conditions. Our ages, however, rule out an Alpine influence on the zircons.

Comparison of Radiometric Ages

The new dating of the eclogitic rocks from the Central Menderes basement (Ödemiş-Kiraz complex) demonstrates a Pan African high-pressure event. This has to fit into the known picture of the Pan-African evolution, and it will be done by comparison with published results (Table 1) from granulites, augen gneisses and migmatites.

Electron microprobe (EMPA) monazite ages of granulites from Tire scatter around 600 Ma (592±26 Ma monazite in garnet; 614±25 Ma in matrix; Warkus 2001). U-Pb SHRIMP zircon analyses of the same locality gave 583.0±5.7 Ma (Koralay *et al.* 2006).

Augen gneiss samples show a wide spread of U-Pb ages, 540–560 Ma (Hetzel & Reischmann 1996; Dannat 1997; Koralay *et al.* 1998, 2001). Monazite EMPA ages from the augen gneiss surrounding the

eclogitic metagabbro near Birgi peak are around 580±35 and 640±45 Ma (>100 measurements; Warkus 2001), while Pb-Pb evaporation ages average at 539±9 Ma (Warkus 2001).

The age of the migmatization and related granites was determined as ~540 Ma in the Gördes area (Dannat 1997), 551±1.4 Ma in the Birgi area (Hetzel *et al.* 1998) and 560.0±15.0 Ma in the Tire area (Koralay *et al.* 2006), respectively.

At Birgi (Ödemiş-Kiraz complex) the age of the coronitic metagabbros (sample 362, 540.4±3.5 Ma), interpreted to be the intrusion age of the gabbroic protolith, is slightly older than the age of the eclogitic metagabbro (sample 361, 529.9±22 Ma) representing the eclogite or eclogite-amphibolite facies transition. No age recording the granulite stage was observed in the zircons. For the Tire area the ²⁰⁶Pb/²³⁸U zircon age of 531±9 Ma is interpreted as its minimum age.

The geological, petrological and textural evidence suggest a relative order for the polyphase metamorphic evolution of the Pan-African basement, with granulite and eclogite stages (Candan *et al.* 2001). Both events are overprinted by a later high-temperature amphibolite facies. This high temperature event caused local migmatization and granite formation in some parts of the Menderes Massif.

In conclusion, the zircon age data from coronitic and eclogitic metagabbros presented here is consistent with geological constraints as well as relative and radiometric ages of the granulites. We infer that metagabbros represent Pan-African intrusions dated as 540 Ma, which shortly after their intrusion underwent an eclogite facies metamorphism (530 Ma).

Relationship with the Mozambique Belt

The Pan-African orogeny, involving a protracted orogenic cycle from 950 to 450 Ma (Kröner 1984), encompasses the processes involved in complete amalgamation of Gondwana. Neoproterozoic plate configurations (Stern 1994; Wilson *et al.* 1997) suggest that East and West Gondwana were separated by a major basin, called the 'Mozambique Ocean' (Dalziel 1991). The closure of this ocean and continental collision of East and West Gondwana resulted in the development of a N–S-trending

orogenic belt (Mozambique belt) exposed along the eastern margin of Africa.

The Mozambique belt is characterized by high-grade metamorphism with granulites. Stern (1994) related granulite facies metamorphism to the closure of the Mozambique Ocean and continental collision of East and West Gondwana. Thus, the age of this metamorphism can be used as direct evidence for the timing of the collision. Present age constraints, including zircon ages of granulites, cluster around 715–650 Ma (Sabaloka-Sudan; Kröner *et al.* 1987; Tanzania; Maboko *et al.* 1989) and 610–520 Ma (ca. 550 Ma) (Madagascar; Paquette *et al.* 1994; India; Choudhary *et al.* 1992; Sri Lanka; Kröner *et al.* 1994).

Stern (1994) considered that the first age group reflects the final collision of East and West Gondwana. The spread in ages was interpreted to be due to irregular shapes of the colliding continental margins (Muhongo 1994). According to these authors, final collision and suturing of East and West Gondwana along the Mozambique belt thus occurred during the late Neoproterozoic (640–680 Ma). However, the tectonic setting of the granulite formation within the Mozambique belt is controversial. As emphasized by Möller *et al.* (2000), the granulite facies metamorphism in Tanzania cannot be attributed to a continent-continent collision setting due to slow cooling rates and low pressure conditions corresponding to a crustal thickness of < 40 km. Similarly, Wilson *et al.* (1997) noted concerns for a tectonic model of the 'older granulites' and envisaged a time range between 600–550 Ma for the culmination of continent-continent collision.

Recently, eclogites from northern Malawi have been reported in the Mozambique belt (Ring *et al.* 2002). This high-pressure event was dated at 530–

500 Ma by the zircon Pb/Pb evaporation method. The eclogite-facies metamorphism was related to crustal thickening during subduction/collision and suggests the timing of the final collision of the Mozambique Ocean was Early Cambrian.

Plate reconstructions place the Menderes and Bitlis massifs, where kyanite-bearing eclogites of Pan-African age were reported (Okay *et al.* 1985) at the northern end of the Mozambique belt in the Cambrian (Şengör *et al.* 1984; Stern 1994; Dora *et al.* 1995; Stampfli & Borel 2002; Gessner *et al.* 2004). The new age data for the Menderes eclogites (530 Ma), consistent with the date of the Malawi eclogites, suggests a genetic connection of the Pan-African basement of the Menderes Massif with the suture of the Mozambique belt. Although direct links between the Menderes Massif and Mozambique belt are obliterated by subsequent plate dispersal the inferred tectonic setting and age of the Menderes eclogites corroborates terminal collision of East and West Gondwana and the final suturing of the Mozambique Ocean during Early Cambrian closure of the Mozambique ocean.

Acknowledgements

We would like to thank O.Ö. Dora for his continuous support of our work. This cooperation was and is substantially supported by the German Science Foundation, DFG (grant OB 80/22), the Volkswagenstiftung, the German academic exchange organization, DAAD, and the 'Deutsch-Französische Hochschule' as well as TÜBİTAK (grant 101Y022). The support of all these granting agencies is warmly acknowledged. We thank Aral Okay and Erdin Bozkurt as well as P. O'Brien and R. Bousquet for critically reading the manuscript.

References

- BOZKURT, E. & OBERHÄNSLI, R. 2001. Menderes Massif (Western Turkey): structural, metamorphic and magmatic evolution – a synthesis. *International Journal of Earth Sciences* **89**, 679–708.
- BOZKURT, E. & SATIR, M. 2000. The southern Menderes Massif (western Turkey): geochronology and exhumation history. *Geological Journal* **35**, 285–296.
- CAMERON, A.E., SMITH, D.H. & WALKER, R.L. 1969. Mass spectrometry of nanogram-size samples of lead. *Nature* **41**, 525–526.
- CANDAN, O., DORA, O.Ö., DÜRR, S. & OBERHÄNSLI, R. 1994. Erster Nachweis von Granulit und Eklogit-Relikten im Menderes Massiv/Türkei. *Göttinger Arbeiten zur Geologie und Paläontologie Sb* **1**, 217–220.

- CANDAN, O. 1996a. Kiraz-Birgi çevresindeki (Menderes Masifi/Ödemiş-Kiraz asması) metagabroların petrografisi ve metamorfizması [Petrography and metamorphism of the metagabbros at the northern part of Alaşehir, Demirci-Gördes submassif of the Menderes Massif]. *Yerbilimleri* **18**, 1–25 [in Turkish with English abstract].
- CANDAN, O. 1996b. Aydın-Çine Asması'ndeki (Menderes Masifi) gabroların metamorfizması ve diğer asmasılarla karşılaştırılması [Metamorphism of the gabbros in the Aydın-Çine submassif and their correlation with those in the related submassifs of the Menderes Massif]. *Turkish Journal of Earth Sciences* **5**, 123–139 [in Turkish with English abstract].
- CANDAN, O., DORA, O.Ö., OBERHÄNSLI, R., ÇETİNKAPLAN, M., PARTZSCH, J.H., WARKUS & F.C. DÜRR, S. 2001. Pan-African high-pressure metamorphism in the Precambrian basement of the Menderes Massif, western Anatolia, Turkey. *International Journal of Earth Sciences* **89**, 793–811.
- CATLOS, E.J. & ÇEMEN, İ. 2005. Monazite ages and the evolution of the Menderes Massif, western Turkey. *International Journal of Earth Sciences* **94**, 204–217.
- ÇETİNKAPLAN, M. 1995. *Geochemical, Mineralogical and Petrographical Investigation of the Eclogites in Southern Part of Tire Area, Ödemiş-Kiraz Submassif of Menderes Massif*. MSc Thesis, Dokuz Eylül University, Graduate School of Nature and Applied Sciences, İzmir, Turkey [unpublished].
- CHOUNDHARY, A.K., HARRIS, N.B.W., VAN CALSTERN, P. & HAWKESWORTH, C.J. 1992. Pan-African charnockite formation in Kerala, south India. *Geological Magazine* **129**, 257–267.
- DALZIEL, I.W.D. 1991. Pacific margins of Laurentia and east Antarctica-Australia as a conjugate rift pair: evidence and implications for an Eocambrian supercontinent. *Geology* **19**, 598–601.
- DANNAT, C. 1997. *Geochemie, Geochronologie und Nd-Sr-Isotopie der granitoiden Kerngneise des Menderes Massivs, SW-Türkei*. Dissertation, Universität Mainz.
- DORA, O.Ö. 1976. Die Feldspäte als petrogenetischer Indikator im Menderes Massiv / Westanatolien. *Neues Jahrbuch für Mineralogie Abhandlungen* **127**, 289–310.
- DORA, O.Ö., CANDAN, O., DÜRR, S. & OBERHÄNSLI, R. 1995. New evidence on the geotectonic evolution of the Menderes Massif. In: *Proceedings of International Earth Sciences Colloquium on the Aegean Region, İzmir, Turkey* **1**, 53–72.
- DORA, O.Ö., CANDAN, O., KAYA, O. & KORALAY, E. 2002. *Menderes Masifi'ndeki Leptit-Gnaysların Kökenlerinin Yeniden Yorumlanması, Metamorfizmaları ve Jeotektonik Ortamları [Protoliths, Tectonic Setting and Metamorphism of the Leptitegneisses in the Menderes Massif]*. TÜBİTAK project (YDABÇAG-554) report [in Turkish with English abstract, unpublished].
- DORA, O.Ö., CANDAN, O., KAYA, O., KORALAY, O.E. & AKAL, C. 2005. *Menderes Masifi Çine Asması'ndeki Koçarlı-Bafa-Yatağan-Karacasu Arasında Uzanan Gnays/Şist Dokanağının Niteliği: Jeolojik, Tektonik, Petrografik ve Jeokronolojik Bir Yaklaşım [The Contact Relationship Between Gneiss and Schist Extending Along Koçarlı, Bafa, Yatağan, Karacasu in Çine Submassif, Menderes Massif: A Geological, Structural, Petrological and Geochronological Approach]*. TÜBİTAK project (YDABÇAG 101Y132) report [in Turkish with English abstract, unpublished].
- DÜRR, S. 1975. *Über Alter und geotektonische Stellung des Menderes-Kristallins/SW-Anatolien und seine Aequivalente in der mittleren Aegaeis*. Habilitation Thesis, University of Marburg/Lahn, Germany.
- GESSNER, K., PIAZOLO, S., GÜNGÖR, T., RING, U., KRÖNER, A. & PASSCHIER, C.W. 2001. Tectonic significance of deformation in granitoid rocks of the Menderes nappes, Anatolide belt, southwest Turkey. *International Journal of Earth Sciences* **89**, 766–780.
- GESSNER, K., COLLINS, A., RING, U. & GÜNGÖR, T. 2004. Structural and thermal history of poly-orogenic basement: U–Pb geochronology of granitoid rocks in the southern Menderes Massif, Western Turkey. *Journal of the Geological Society, London* **161**, 93–101.
- GESSNER, K., RING, U., PASSCHIER, C.W. & HETZEL, R. 2002. Discussion on 'Stratigraphic and metamorphic inversions in the central Menderes Massif: a new structural model', by Aral I. Okay. *International Journal of Earth Sciences* **91**, 168–172.
- HETZEL, R., PASSCHIER, C.W., RING, U. & DORA, O.Ö. 1995. Bivergent extension in orogenic belts; the Menderes Massif (southwestern Turkey). *Geology* **23**, 455–458.
- HETZEL, R. & REISCHMANN, T. 1996. Intrusion age of Pan-African augen gneisses in the southern Menderes Massif and the age of cooling after Alpine ductile extensional deformation. *Geological Magazine* **133**, 565–572.
- HETZEL, R., ROMER, R.L., CANDAN, O. & PASSCHIER, C.W. 1998. Geology of the Bozdağ area, central Menderes Massif, SW Turkey: Pan-African basement and alpine deformation. *Geologische Rundschau* **87**, 394–406.
- JAFFEY, A.H., FLYNN, K.F., GLENDENIN, L.E., BENTLEY, W.C. & ESSLING, A.M. 1971. Precision measurement of half-lives and specific activities of ^{235}U and ^{238}U . *Physical Review (C)* **4**, 1889–1906.
- KORALAY, E.O., SATIR, M. & DORA, O.Ö. 1998. Geochronologic evidence of Triassic and Precambrian magmatism in the Menderes Massif, west Turkey. *Third International Turkish Geological Symposium Abstracts*, p. 285
- KORALAY, E.O., SATIR, M. & DORA, O.Ö. 2001. Geochemical and geochronological evidence for Early Triassic calc-alkaline magmatism in the Menderes Massif, western Turkey. *International Journal of Earth Sciences* **89**, 822–835.

- KORALAY, E., DORA, O.Ö., CHEN, F., SATIR, M. & CANDAN, O. 2004. Geochemistry and geochronology of orthogneisses in the Derbent (Alaşehir) area, Eastern part of the Ödemiş-Kiraz submassif, Menderes Massif: Pan-African magmatic activity. *Turkish Journal of Earth Sciences* **13**, 37–61.
- KORALAY, E.O., CHEN, F., OBERHÄNSLI, R., WAN, Y. & CANDAN, O. 2006. Age of granulite facies metamorphism in the Menderes Massif, Western Anatolia / Turkey: SHRIMP U-Pb Zircon Dating. *Abstracts of 59th Turkish Geological Kurultai*, 28–29.
- KORALAY, E., CANDAN, O., DORA, Ö., SATIR, M., OBERHÄNSLI, R. & CHEN, F. 2007. Menderes Masifi'ndeki Pan-Afrikan ve Triyas yaşlı metamagmatik kayaların jeolojisi ve jeokronolojisi, Batı Anadolu, Türkiye [Geology and geochronology of the Pan-African and Triassic metamagmatic rocks in the Menderes Massif, W-Anatolia, Turkey]. *Menderes Masifi Kolokyumunu, İzmir*, 18–24.
- KROGH, T.E. 1973. A low-contamination method for hydrothermal decomposition of zircon and extraction of U and Pb for isotopic age determination. *Geochimica et Cosmochimica Acta* **37**, 485–494.
- KRÖNER, A. 1984. Late Precambrian plate tectonics and orogeny: a need to redefine the term Pan-African. In: KLERKX, J. & MICHOT, J. (eds), *African Geology Tervuren*. Musée R. l'Afrique Centrale, 23–28.
- KRÖNER, A., STERN, R.J. & DAWOUD, S.S. 1987. The Pan-African continental margin in northeastern Africa: evidence from a geochronological study of granulites at Sabaloka, Sudan. *Earth Planetary Science Letters* **85**, 91–104.
- KRÖNER, A., JAECKEL, P. & WILLIAMS, I.S. 1994. Pb loss patterns in zircons from a high-grade metamorphic terrain as revealed by different dating methods: U-Pb and Pb-Pb ages for igneous and metamorphic zircons from northern Sri Lanka. *Precambrian Research* **66**, 151–181.
- LIPS, A.L.W., CASSARD, D., SÖZBİLİR, H., YILMAZ, H. & WIJBRANS, J.R. 2001. Multistage exhumation of the Menderes Massif, western Anatolia (Turkey). *International Journal of Earth Sciences* **89**, 781–792.
- LOOS, S. & REISCHMANN T. 1999. The evolution of the southern Menderes Massif in SW Turkey as revealed by zircon dating. *Journal of the Geological Society, London* **156**, 1021–1030.
- LUDWIG, K.R. 1980. Calculation of uncertainties of U-Pb isotope data. *Earth Planetary Science Letters* **46**, 212–220.
- MABOKO, M.A.H., MCDUGALL, I. & ZEITLER, P.K. 1989. Dating Late Pan-African cooling in the Uluguru granulite complex of eastern Tanzania using ⁴⁰Ar-³⁹Ar technique. *Journal of African Earth Sciences* **9**, 159–167.
- MÖLLER, A., MEZGER, K. & SCHENK, V. 2000. U-Pb dating of metamorphic minerals: Pan-African metamorphism and prolonged slow cooling of high pressure granulites in Tanzania, East Africa. *Precambrian Research* **104**, 123–146.
- MUHONGO, S. 1994. Neoproterozoic collision tectonics in the Mozambique belt of East Africa: evidence from the Uluguru mountains, Tanzania. *Journal of African Earth Sciences* **19**, 153–168.
- OBERHÄNSLI, R., CANDAN, O., DORA, O.Ö. & DÜRR, ST. 1997. Eclogites within the Menderes Massif/western Turkey. *Lithos* **41**, 135–150.
- OBERHÄNSLI, R., WARKUS, F. & CANDAN, O. 2002. Dating of eclogite and granulite facies relics in the Menderes Massif. *Abstracts, First International Symposium of the Faculty of Mine (İTÜ) on Earth Sciences and Engineering, İstanbul, Turkey*, p. 104.
- OKAY, A.I., ARMAN, M.B. & GÖNCÜOĞLU, M.C. 1985. Petrology and phase relations of the kyanite-eclogites from eastern Turkey. *Contributions to Mineralogy and Petrology* **91**, 196–204.
- PAQUETTE, J.L., NEDELEC, A., MONIE, P. & RAKOTONDRAZAFY, M. 1994. U-Pb single zircon Pb-evaporation and Sm-Nd isotopic of granulitic domain in SE Madagascar. *Journal of Geology* **102**, 523–538.
- PARTZSCH, J.H., OBERHÄNSLI, R., CANDAN, O. & WARKUS F.C. 1998. The evolution of the Central Menderes Massif, West Turkey: a complex nappe pile recording 1.0 Ga of geological history. *Freiberger Forschungshefte C-471*, 166–168.
- REISCHMANN, T., KRÖNER, A., TODT, W., DÜRR, S. & ŞENGÖR, A.M.C. 1991. Episodes of crustal growth in the Menderes Massif, W. Turkey. *Terra Nova Abstracts*, p. 34.
- RIMMELÉ, G., OBERHÄNSLI, R., GOFFÉ, B., JOLIVET, L., CANDAN, O. & ÇETİNKAPLAN., M. 2003. First evidence of high-pressure in the 'cover series' of the southern Menderes Massif. Tectonic and metamorphic implications for the evolution of SW Turkey. *Lithos* **71**, 19–46.
- RING, U., KRÖNER, A., BUCHWALD, R., TOULKERIDIS, T. & LATER, P. 2002. Shear zone patterns and eclogite-facies metamorphism in the Mozambique belt of northern Malawi, east-central Africa: implication for assembly of Gondwana. *Precambrian Research* **116**, 19–56.
- RING, U., LAWS, S. & BERNET, M. 1999a. Structural analysis of a complex nappe sequence and late-orogenic basins from the Aegean Island of Samos, Greece. *Journal of Structural Geology* **21**, 1575–1601.
- RING, U., GESSNER, K., GÜNGÖR, T. & PASSCHIER, C.W. 1999b. The Menderes Massif of Western Turkey and the Cycladic Massif in the Aegean – do they really correlate? *Journal of the Geological Society, London* **156**, 3–6.
- SCHUILING, R.D. 1973. Active role of continents in tectonic evolution, geothermal modals. In: De Jong K.A. And R. Scholten (Eds): *Gravity and tectonics*. New York, 37–47.
- SATIR, M. & FRIEDRICHSEN, H. 1986. The origin and evolution of the Menderes Massif, W-Turkey: A rubidium/ strontium and oxygen isotope study. *Geologische Rundschau* **75**, 703–714.
- ŞENGÖR, A.M.C., SATIR, M. & AKKÖK, R. 1984. Timing of tectonic events in the Menderes Massif, western Turkey: implications for tectonic evolution and evidence for Pan-African basement in Turkey. *Tectonics* **3**, 693–707.
- STACEY, S. & KRAMERS, J.D. 1975. Approximation of terrestrial lead isotope evolution by a two-stage model. *Earth and Planetary Science Letters* **26**, 207–221.

- STAMPFLI, G.M. & BOREL, G.D. 2002. A plate tectonic model for the Paleozoic and Mesozoic constrained by dynamic plate boundaries and restored synthetic oceanic isochrones. *Earth and Planetary Science Letters* **196**, 17–33.
- STEIGER, R.H. & JÄGER, E. 1977. Subcommission geochronology: convention on the use of decay constants in geo- and cosmochronology. *Earth and Planetary Science Letters* **36**, 359–362.
- STERN, R.J. 1994. Arc assembly and continental collision in the Proterozoic east African orogen: implications for the consolidation of Gondwanaland. *Annual Review of Earth and Planetary Sciences* **22**, 319–351.
- VAVRA, G., SCHMID, R. & GEBAUER, D. 1999. Internal morphology, habit and U-Th-Pb microanalysis of amphibolite-to-granulite facies zircons: geochronology of the Ivrea Zone (Southern Alps). *Contributions to Mineralogy and Petrology* **134**, 380–404.
- WARKUS, F.C. 2001. *Untersuchungen an Hochdruckrelikten im zentralen Menderes Massiv, W Türkei*. Dissertation, Universität Potsdam.
- WHITNEY, D.L., TEYSSIER, C., KRUCKENBERG, S.C., MORGAN, V.L. & IREDALE, L.J. 2008. High-pressure–low-temperature metamorphism of metasedimentary rocks, southern Menderes Massif, western Turkey. *Lithos* **101**, 218–232.
- WILSON, T.J., GRUNOW, A.M. & HANSON, R.E. 1997. Gondwana assembly: The view from southern Africa and east Gondwana. *Journal of Geodynamics* **23**, 263–286.